reducing ammonium ion concentrations. The calculated activation energies are 7.5 kcal at 1.3 m*M* urea and 9.5 kcal at 1.3 *M* urea. These correspond very well with the data obtained in Tris buffer, both in terms of magnitude and the direction in which they change.

Summary

The products of the hydrolysis of urea catalyzed by urease have been determined calorimetrically in four buffer systems. Two of these (phosphate and maleate) yield the classical products NH_4^+ and HCO_3^-, while the other two (citrate and Tris) give an almost quantitative yield of ammonium carbamate.

Additional, qualitative studies show that the formation of the classical products from ammonium carbamate is a nonenzymatic process dependent solely upon the nature of the buffer. This reinforces the ammonium carbamate concept (especially considering the low pH at which the results were obtained) and also suggests that rather than being an intermediate, ammonium carbamate is the true product of this enzymatic process.

Several buffer effects are discussed. Two are found to be readily explained on the basis of ammonium ion inhibition. The third, involving the change in optimum pH with buffer, is perhaps the only true buffer effect, involving a unique example of simultaneous general acid and general base catalysis.

Acknowledgment. Appreciation is expressed to the Robert Welch Foundation for its support of this work through Grant F-537. J. Neil Baldridge, W. Michael Breland, and Donna Chesluk generated much of the data upon which this report is based.

References and Notes

(1) S. F. Howell and J. B. Sumner, *J. Biol. Chem.*, **104,** 619 (1934).
(2) M. C. Wall and K. J. Laidler, *Arch. Biochem. Biophys.*, **43,** 299 (1953).
(3) K. J. Laidler and J. P. Hoare, *J. Am. Chem. Soc.*, **71,** 2699 (1949).
(4) K. J. Laidler and J. P. Hoare, *J. Am. Chem. Soc.*, **72,** 2489 (1950).
(5) F. J. Reithel in "The Enzymes," Vol. IV, P. D. Boyer, Ed., Academic Press, New York, N.Y., 1971, Chapter 1.
(6) R. D. Rossini, D. D. Wagman, W. H. Evans, S. Levine, and I. Jaffe, *Nat. Bur. Stand. (U.S.), Circ.*, **No. 500** (1952).
(7) R. M. Izatt and J. J. Christensen in "Handbook of Biochemistry," R. C. Weast, Ed., Chemical Rubber Publishing Co., Cleveland, Ohio, 1968, p J-49.
(8) J. B. Sumner, D. B. Hand, and R. G. Halloway, *J. Biol. Chem.*, **91,** 331 (1931).
(9) R. L. Blakeley, J. A. Hinds, H. E. Kunze, E. C. Webb, and B. Zerner, *Biochemistry*, **8,** 1991 (1969).
(10) K. Hanabusa, *Nature (London)*, **189,** 551 (1961).
(11) N. D. Jespersen and J. Jordan, *Anal. Lett.*, **3,** 323 (1970).
(12) J. H. Wang and D. A. Tarr, *J. Am. Chem. Soc.*, **77,** 6205 (1955).
(13) M. Hanss and A. Rey, *Biochim. Biophys. Acta*, **227,** 630 (1971).
(14) J. P. Hoare and K. J. Laidler, *Can. J. Biochem.*, **48,** 1132 (1970).
(15) K. J. Laidler, "The Chemical Kinetics of Enzyme Action," Oxford University Press, London, 1958, pp 87–95.
(16) G. H. Ayres, *Anal. Chem.*, **21,** 652 (1949).
(17) P. V. Sundaram and K. J. Laidler, *Can. J. Biochem.*, **48,** 1132 (1970).
(18) G. B. Kistiakowsky and A. J. Rosenberg, *J. Am. Chem. Soc.*, **74,** 5020 (1952).

Luminescence and Simplified Photophysics of Methylglyoxal

R. A. Coveleskie and James T. Yardley* †

Contribution from the Department of Chemistry, University of Illinois, Urbana, Illinois 61801.

Received August 5, 1974

Abstract: Steady state spectra and time-resolved luminescence decays have been observed for methylglyoxal. Absorption spectra ascribed to the $^1A''(^1A_u^1) \leftarrow {}^1A'(^1A_g^1)$ transition have been described and the 0-0 band assigned to be at either 22,260 or 22,090 cm^{-1}. Several vibrational progressions in ~270–280 cm^{-1} have also been observed. The emission spectra indicate the presence of the $^3A''(^3A_u^1)$ state approximately 2400 cm^{-1} lower in energy from the $^1A''(^1A_u^1)$ level. A simple kinetic scheme is presented which explains the behavior of the relative intensities of fluorescence and phosphorescence as well as the luminescence decay behavior for methylglyoxal pressures above ~2.0 Torr. Below 2.0 Torr more complicated behavior may occur due to the reversible nature of the S_1–T_1 coupling.

Extensive examinations of photophysical and photochemical behavior for low-lying excited electronic states of the simple dicarbonyl molecules glyoxal[1-4] (HCOCHO) and biacetyl[5-9] [$CH_3COC(CH_3)O$] have been recently carried out. We report here absorption spectra, emission spectra, and time-resolved luminescence decays for methylglyoxal (pyruvaldehyde, CH_3COCHO) which is structurally intermediate to glyoxal and biacetyl. We also present a simplified kinetic scheme which describes the observed luminescence behavior for total pressures above ~2 Torr. Such an investigation is of considerable importance for several reasons.

(1) Only two ($^1A_u^1$, commonly denoted S_1, and $^3A_u^1$, commonly denoted T_1) of the eight low-energy n,π^* excited electronic states expected for *trans*-dicarbonyl systems have been observed and definitively assigned in gaseous glyoxal and biacetyl. The reduction of C_{2h} to C_s symmetry formally allows transitions between the ground state and the other n,π^* excited singlet states, opening the possibility for the direct spectroscopic observation of these states and thus leading to a better definition of the photophysical possibilities of the $^1A_u^1$ state.

(2) Finlayson, Pitts and Atkinson[10] have recently observed chemiluminescence from reactions of isobutene, 2-methyl-2-butene, and 2,3-dimethyl-2-butene with 2% O_3 in O_2. Part of the chemiluminescence spectrum closely corresponds to that observed in this work. A characterization of the luminescence features is necessary for the reliable interpretation of such photochemical data and for reliable product identification.

(3) Recent photophysical experiments on biacetyl and glyoxal have revealed a number of striking differences in behavior.[1,2,6,7] Examination of corresponding behavior in methylglyoxal may provide insight concerning the changing photophysical behavior in these systems.

Experimental Section

Chemicals. Methylglyoxal (40% aqueous solution) was obtained from Aldrich Chemical Co. In order to obtain pure methylglyoxal the sample was first vacuum distilled to increase the methylglyoxal

† Alfred P. Sloan Fellow, 1972–1974.

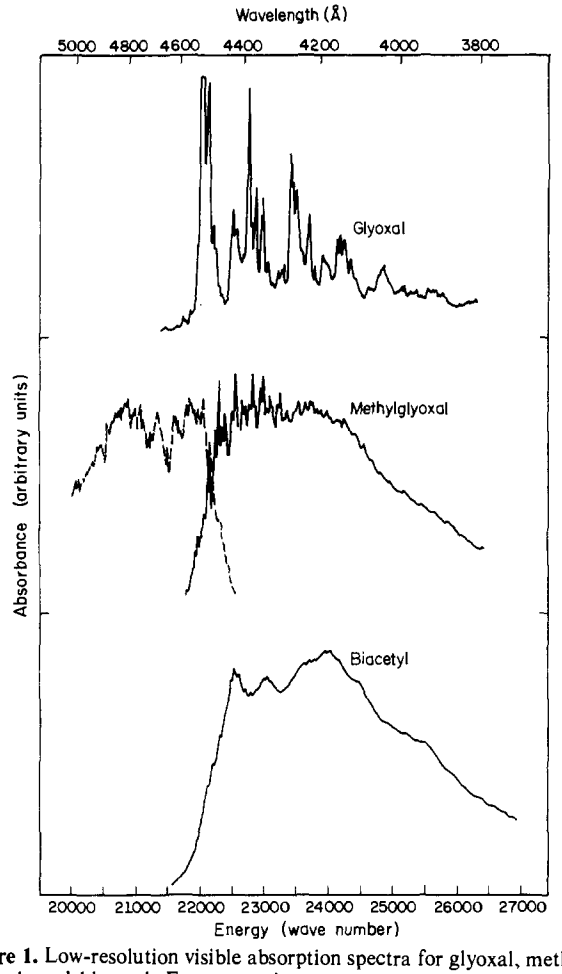

Figure 1. Low-resolution visible absorption spectra for glyoxal, methylglyoxal, and biacetyl. For comparison purposes, a portion of the observed emission spectrum of methylglyoxal is also displayed (dashed lines).

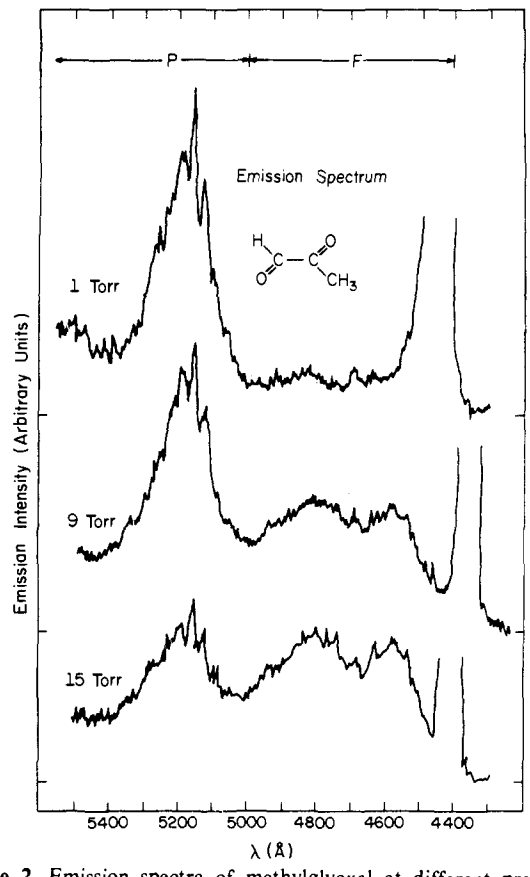

Figure 2. Emission spectra of methylglyoxal at different pressures. Slightly different excitation wavelengths, λ_{EX}, and bandwidths ($\Delta\lambda$) were used: λ_{EX} = 4450 Å, $\Delta\lambda \sim$ 100 Å for 1.00 Torr; λ_{EX} = 4360 Å, $\Delta\lambda \sim$ 75 Å for 9.0 Torr; and λ_{EX} = 4410 Å, $\Delta\lambda \sim$ 75 Å for 15.0 Torr. The spectral extent of the two emission regions, F and P, is also shown (see text). Region P extends to ~6200 Å.

concentration. Commercial "aquasorb," in an amount equal to one-half the sample volume, was added. After degassing, the sample was heated to ~70–90°. A Dry Ice–acetone bath was used to trap water vapor and methylglyoxal was collected in a trap cooled to −196°. In some preparations an additional trap at −21° preceded the Dry Ice–acetone bath. The sample was then pumped on at Dry Ice temperature. Mass spectra and NMR spectra of the final product showed no trace of water, glyoxal, biacetyl, or any other impurity. Samples were stored at −196°. Some deterioration with repeated warmings was observed as evidenced by a decrease in emission intensity of sample vapor and the growth of higher mass number peaks (around mass 145) in mass spectra. Linde high purity Ar (99.996%) was used. Biacetyl[6] and glyoxal[1] were prepared as described previously.

Absorption Spectra. The low-resolution absorption spectra were recorded on a Cary 14 spectrometer using an 11.9 cm long Pyrex tube with quartz windows as the sample cell. High-resolution spectra were obtained from an 8 m Czerny-Turner mount spectrometer described previously.[11] The greaseless high-vacuum system and associated pressure measuring devices have been discussed previously.[12]

Emission Spectra. Steady state emission spectra were recorded on a Spex 1700-III spectrometer (0.75 m Czerny-Turner; 1200 l./mm grating) with ~10 Å resolution. The excitation source was a 1000 W Xenon arc lamp coupled through a ¼-m Jarrell Ash monochromator. Excitation bandwidths were ~100 Å. A cooled (−20°) RCA C31034A photomultiplier tube generated the photocurrent which was recorded on chart paper. This tube is particularly appropriate due to its relatively constant quantum efficiency from 3000 to 8500 Å. The background pressure in the fluorescence cell was 10^{-6} Torr. The gas pressure was measured with various transducers.

Time-Resolved Luminescence. The apparatus used in the vapor phase time resolved experiments has been described previously.[12] A N_2-laser pumped dye laser (4 nsec FWHM) was used as the light source. The active laser medium was a solution of 7-diethylamino-4-methylcoumarin (~5 × 10^{-2} *M* in EtOH). All time-resolved experiments reported here utilized an excitation wavelength of 4492 ± 0.5 Å ($\Delta\lambda$ < 0.5 Å).

The dye laser beam was directed by means of a set of mirrors to a fluorescence cell described previously.[12] The luminescence was monitored through a set of baffles by RCA C31000A or 8575 photomultiplier tubes. Appropriate Corning glass filters or dielectric filters were interposed between the fluorescence cell and photomultiplier tube to eliminate scattered laser light. Decays were observed on both nsec and msec time scales, requiring different methods of analysis.

For the nsec decay, the photomultiplier tube was connected directly to a Tektronix 454 oscilloscope (150 MHz, 50 Ω termination). Luminescence decays were photographed, averaged, and digitized. The emission $1/e$ lifetime, τ, and the corresponding rate constant, $k = \tau^{-1}$, were determined by a least-square fit of the form: $\ln I(t) = \ln I(0) - t/\tau$, where $I(t)$ is the emission intensity at time t.

For the msec decays the photomultiplier tube was connected through a 500 Ω resistor in parallel with a capacitance of 50–400 pF (RC = 0.025–0.2 μsec) to a Biomation Model 610 transient recorder (6-bit accuracy and 0.2 msec time resolution). The digital representation of the luminescence intensity versus time was read into a PDP 8/e computer for on-line signal averaging.

Results

Absorption Spectra. A low-resolution absorption spectrum of methylglyoxal is shown in Figure 1. For comparison spectra of biacetyl and glyoxal are also shown. The lowest energy observed transition occurs in the region 4600–3500 Å (21,739–28,571 cm^{-1}). Another absorption band, with similar oscillator strength, originates at ~3500 Å (30,300

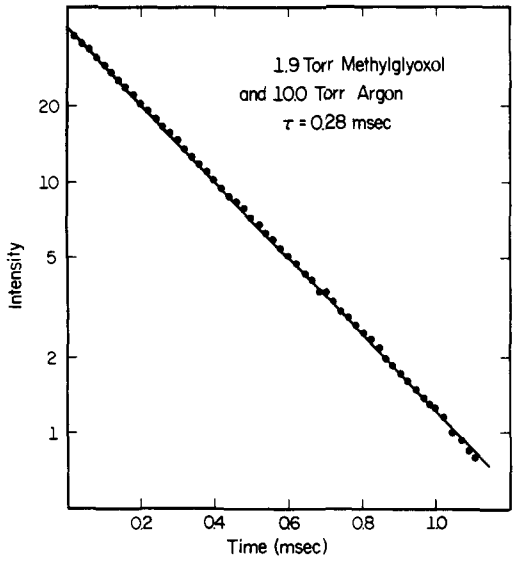

Figure 3. Semilogarithmic plot of the intensity of emission attributed to region P against time for methylglyoxal pressure of 1.9 Torr in 10.0 Torr of argon.

cm^{-1}) and extends to higher energy. Some structure is discernible in the region from 4600 to 4300 Å. For wavelengths shorter than 4300 Å, the spectrum becomes increasingly diffuse.

Emission Spectra. Figure 2 displays the observed emission spectra for varying amounts of methylglyoxal ($\lambda_{exc} \sim$ 4350-4450 Å, $\Delta\lambda \sim$ 100 Å). Two distinct regions of light emission are observed. The intensity of emission occurring mainly in the region 4400-5000 Å (region F) increases with increasing methylglyoxal pressure. On the other hand emission occurring in the region 5000-6200 Å (region P) increases rapidly to ~1 Torr and then remains relatively constant at higher pressures. The emission intensity ratios (I_F/I_P), i.e., ratio of areas under the respective emission components, are 0.11, 0.10, 0.17, 0.66, and 1.17 for methylglyoxal pressures of 0.5, 1.0, 2.0, 9.0, and 15.0 Torr, respectively. The listed ratios include corrections due to overlap of emission components around 5000 Å. The spectral extent of region P is determined from low-pressure data and the spectral envelope of region F determined from high-pressure emission. The low-pressure ratios have a greater degree of inaccuracy due to difficulty in effectively extracting the fluorescence areas. Some structure is evident in both F and P regions.

Luminescence Decay. For methylglyoxal pressures above 2 Torr, two exponential decays are observed. Using a 3-69 Corning filter (10% T at 5200 Å, 1% T at 5100 Å) a msec decay is observed. A nsec decay is also observed with a 3-71 Corning filter (10% T at 4670 Å, 1% T at 4600 Å). With a Corion dielectric filter (central wavelength 4795 Å, half-bandwidth 102 Å), the intensity ratio of the msec decay to the nsec decay is dramatically reduced relative to that observed with the Corning 3-71 filter. Thus, the msec decay apparently originates from spectral region P and the nsec decay from region F.

A typical plot of ln $I(t)$ vs. t for the msec decay is shown in Figure 3. The decay is purely exponential for at least two lifetimes. The addition of up to 200 Torr of Ar to fixed methylglyoxal pressure has less than 1% effect on the observed lifetime. In subsequent experiments on the msec decay, 10 Torr of Ar was added to ensure vibrational equilibration of emitting molecules, and to eliminate any effects due to wall collisions, or diffusion from the viewing area.[13] A plot of the observed rate constant, k, versus methylglyoxal pressure gives a straight line indicating Stern-Volmer behavior (Figure 4). From the intercept of this plot, a collision-free lifetime of 1.92 msec is obtained; from the slope, an effective hard sphere collision cross section of 0.0116 Å^2 may be calculated.

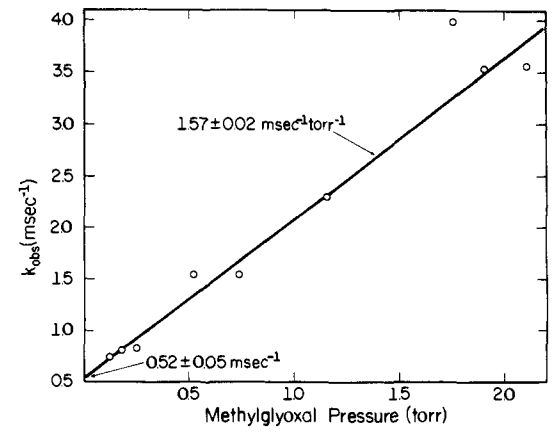

Figure 4. Stern-Volmer plot of methylglyoxal in 10.0 Torr of argon. The calculated quenching cross section is 0.0116 Å^2.

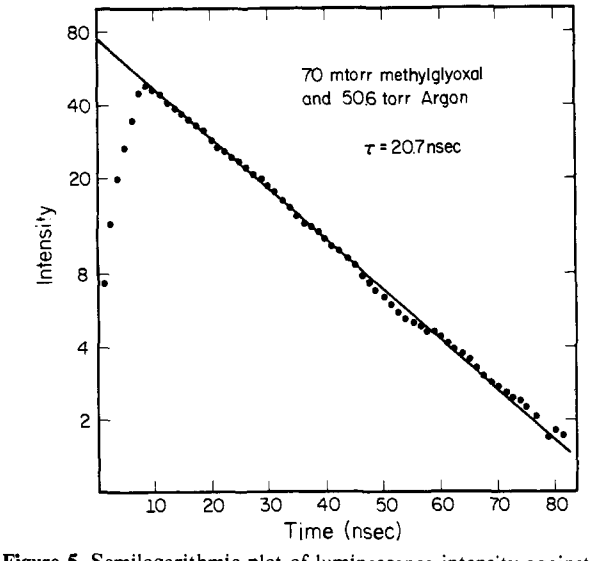

Figure 5. Semilogarithmic plot of luminescence intensity against time of emission attributed to region F for 70 mTorr of methylglyoxal in 50.6 Torr of argon. This decay represents an average of 20 oscilloscope traces.

Figure 5 displays a typical nsec decay (such simple behavior is observed only at pressures above ~2 Torr). The finite risetime of the decay is due both to the finite pulse length of the laser (4 nsec full width at half-mean height), and the finite response time of the corresponding electronics (single photon pulse ~5 nsec full width at half-mean height). The risetime problem has been discussed by McClelland and Yardley.[6] Above ~2 Torr of methylglyoxal simple exponential decay is observed. Below 2 Torr of methylglyoxal, a more complicated decay is observed which will be discussed elsewhere. Figure 6 displays the effect of added Ar pressure to 70 mTorr of methylglyoxal. A collision free lifetime ~20.4 nsec and a quenching cross section <0.08 Å^2 is obtained. Methylglyoxal has been found to be about twice as effective in quenching of the observed rate constant for pressures ranging from 0.07 to 10 Torr. In either case the effect is slight (<~3.0% change in rate constant for added argon pressures from ~0 to 75 Torr).

Discussion

Electronic States. The low-energy electronic states of the trans $(CO)_2$ skeleton have been discussed previously.[14]

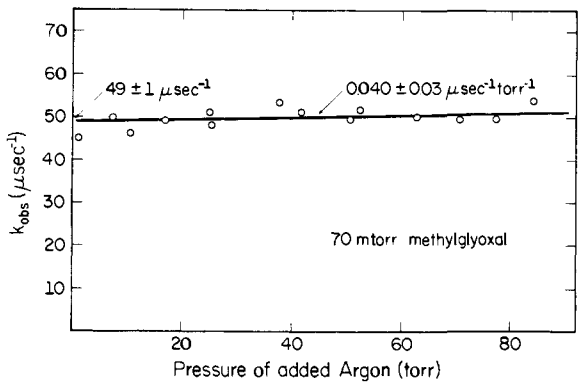

Figure 6. Observed rate constant (k_{obsd}) *vs.* added argon pressure to 70 mTorr of methylglyoxal for the nsec decay. The collision cross-section is <0.08 Å^2.

Since the atomic orbitals situated on the OCCO skeleton comprise the principal basis for the formation of those molecular orbitals involved in the low-lying electronic states, direct correlations of electronic energy levels can be made for glyoxal, methylglyoxal, and biacetyl. Under C_{2h} symmetry, the ground state may be designated as $^1A_g^I(\pi_1{}^2\pi_2{}^2n_+{}^2n_-{}^2)$ and low-lying n,π^* excited states as $^{1,3}A_u^I(\pi_1{}^2\pi_2{}^2n_+{}^1n_-{}^2\pi_3{}^1)$, $^{1,3}B_g^I(\pi_1{}^2\pi_2{}^2n_+{}^2n_-{}^1\pi_3{}^1)$, $^{1,3}B_g^{II}(\pi_1{}^2\pi_2{}^2n_+{}^1n_-{}^2\pi_4{}^1)$, and $^{1,3}A_u^{II}(\pi_1{}^2\pi_2{}^2n_+{}^2n_-{}^1\pi_4{}^1)$ states. Since these excited states are n,π^* in character, the singlet-triplet separation should be small (<3000 cm^{-1}).[15] The absorptions in biacetyl and glyoxal have been definitively assigned as $^1A_u^I \leftarrow {}^1A_g^I$ transitions. Corresponding fluorescence $^1A_u^I \rightarrow {}^1A_g^I$ and phosphorescence $^3A_u^I \rightarrow {}^1A_g^I$ have also been assigned. The absorption of methylglyoxal shown in Figure 1 clearly corresponds to the $^1A_u^I \leftarrow {}^1A_g^I$ absorptions in biacetyl and glyoxal and thus we may confidently assign this absorption to $^1A''(^1A_u^I) \leftarrow {}^1A'(^1A_g^I)$. The luminescence region F, whose origin is at ~22,100 cm^{-1}, shows a reasonably close mirror-image relationship to the $^1A'' \leftrightarrow {}^1A'$ absorption (Figure 1) and thus most likely corresponds to the $^1A''(^1A_u^I) \rightarrow {}^1A'(^1A_g^I)$ fluorescence. The origin of region P luminescence is approximately 2400 cm^{-1} below that of region F. In analogy to luminescence spectra of glyoxal and biacetyl, this almost certainly corresponds to $^3A''(^3A_u^I) \rightarrow {}^1A'(^1A_g^I)$ phosphorescence.

The energies of the remaining n,π^* excited states in glyoxal and biacetyl have not been definitely determined.[14] Of these, the $^1A_u^{II}$ state should lie highest in energy. The ordering of the remaining states should depend upon the magnitude of the splittings of the n_+ and n_- orbitals and of the π_3 and π_4 orbitals. Recent theoretical considerations[16] indicate that the n_+ and n_- orbitals may be separated by as much as 2 eV in contrast to earlier suppositions that this splitting is much smaller.

In glyoxal, an absorption band originating at ~30,000 cm^{-1} has been observed, with an oscillator strength much less than the $^1A_u^I \leftarrow {}^1A_g^I$ band in the low-pressure vapor. This absorption band, once thought to be[17] the dipole-allowed $^1A_u^{II} \leftarrow {}^1A_g^I$ transition, has been recently assigned[18,19] as $^1B_g^{II} \leftarrow {}^1A_g^I$. If this assignment is correct, the oscillator strength likely results from vibronic coupling since the transition is electric-dipole forbidden under C_{2h} symmetry. It is therefore reasonable to suggest that the absorption observed in methylglyoxal near 30,000 cm^{-1} corresponds to the $^1A''(^1B_g^{II}) \leftrightarrow {}^1A'(^1A_g^I)$ transition. Since this transition is not symmetry forbidden in methylglyoxal, it could have considerably higher oscillator strength (relative to the $^1A_u^I \leftarrow {}^1A_g^I$) than in glyoxal, as observed. The failure to observe any additional absorption features between 6500 and 3500 Å indicates that absorptions involving additional n,π^* singlet states are located at still higher energies. If our assignment is correct, we may estimate that the $^1B_g^{II}$ state lies at ~27,000 cm^{-1}, and should be energetically inaccessible for excitation wavelengths longer than ~3700 Å. These results are inconsistent with the suggestions of Drent and Kommandeur[8] and Kaya, Harshbarger, and Robin,[20] which have been discussed recently.[7] The remainder of this paper will deal exclusively with the $^{1,3}A_u^I$ states.

Vibronic Structure. Two features appear in the absorption and emission spectra which might be attributable to the band origin of the $^1A'' \leftrightarrow {}^1A'$ transition (see Figure 1). The most prominent feature is at 4492 Å (22,260 cm^{-1}). However, a "mirror image" relationship between absorption and luminescence would appear to be best satisfied by the weaker feature at 4527 Å (22,090 cm^{-1}). If the potential surfaces of the $^1A'$ and $^1A''$ states are only slightly displaced, as in the case of glyoxal,[21] then the band origin should be the most intense feature in the absorption spectrum. An apparent progression of frequency 273 cm^{-1} originates at 4492 Å. Other progressions of similar frequency are readily apparent. Although it is difficult to build progressions around 4527 Å, this certainly cannot be ruled out as the band origin.

The increasing diffuseness in absorption spectra for the series glyoxal, methylglyoxal, biacetyl may be attributable to two major sources as discussed by Byrne and Ross:[22] (1) "trivial" diffuseness, i.e., simple spectral congestion arising from the addition of vibrational degrees of freedom and (2) "intrinsic" diffuseness, arising from a perturbative interaction which results in the dilution of the oscillator strength over a broader spectral interval. It is, however, difficult to differentiate between these two cases and both effects may well contribute to the diffuseness of absorption in biacetyl and methylglyoxal. Distinct sharp features are observable under high resolution at wavelengths as short as 4304 Å (23,234 cm^{-1}) in the methylglyoxal spectrum.

The emission spectra also exhibit some vibronic structure. Of particular distinction are the features at 19,268 cm^{-1} (5190 Å), 19,395 cm^{-1} (5156 Å), and 19,534 cm^{-1} (5122 Å) in the phosphorescence emission.

Luminescence Decay. It is apparent that emission in region F[$^1A''(^1A_u^I) \rightarrow {}^1A'(^1A_g^I)$] at pressures above ~2 Torr decays exponentially on a nsec timescale. Since the radiative decay rate for this state is expected to be ~10^5 sec^{-1}, the primary decay path would appear to be nonradiative. In analogy to biacetyl and glyoxal, the most likely candidate for major nonradiative interaction is $^1A''(^3A_u^I, T_1)$. The nsec decay, relatively independent of pressure in the region 3 Torr to 75 Torr for excitation at 4492 Å, is reminiscent of the essentially irreversible unimolecular decay found for the corresponding state of biacetyl.[6,9] For glyoxal, it may be noted that this nonradiative interaction is primarily collision induced.[1,4] More detailed discussion will be published elsewhere. The slight change in decay rate with the addition of Ar may well be due to vibrational equilibration.

The msec lifetime ascribed to luminescence of region P is characteristic of phosphorescence decay from the $^3A''(^3A_u^I)$ state. The "zero pressure" lifetime of 1.92 msec may be compared to 3.25 msec for glyoxal[2] and 1.87 msec for biacetyl.[7] It is also interesting to compare the cross section for self-quenching of methylglyoxal (σ = 0.012 Å^2) with that of glyoxal (σ = 0.077 Å^2) and biacetyl ($\sigma < 2 \times 10^{-6}$ Å^2). It has been recently suggested that self-quenching in glyoxal involves the production of some sort of intermediate species. In view of the results reported here, it appears that the presence of an aldehyde proton may be necessary in the formation of such an intermediate. It should be pointed out that the 1.92 msec lifetime for the $^3A''(^3A_u^I)$ state is not necessarily radiative and may well include con-

siderable contribution from $^3A''(^3A_u^I) \rightsquigarrow {}^1A'(^1A_g^I)$ intersystem crossing. This intersystem crossing rate has recently been considered by Moss and Yardley[7] and has been shown to increase rapidly with vibrational excitation for biacetyl.

Simplified Kinetic Scheme. We present here a simplified kinetic scheme which will explain the observed time resolved and steady state luminescence behavior for pure glyoxal at pressures above ~2 Torr. The specific processes included are

excitation

$$S_0 + h\nu \xrightarrow{I_{EX}} S_1 \quad (1)$$

fluorescence

$$S_1 \xrightarrow{k_F} S_0 + h\nu_F \quad (2)$$

intersystem crossing

$$S_1 \xrightarrow{k_{ISC}} T_1 \quad (3)$$

radiationless decay

$$T_1 \xrightarrow{k_X} S_0 \text{ or products} \quad (4)$$

phosphorescence

$$T_1 \xrightarrow{k_P} S_0 + h\nu_P \quad (5)$$

self-quenching

$$T_1 + S_0 \xrightarrow{k_{MT}} \text{products} \quad (6)$$

where S_0, S_1, and T_1 represent the $^1A'(^1A_g^I)$, $^1A''(^1A_u^I)$, and $^3A''(^3A_u^I)$ states respectively, and I_{EX} is the rate of excitation.

Solving the rate equations for the above processes with constant excitation rate gives $I_F = k_F I_{EX}[MG](k_F + k_{ISC})^{-1}$ and $I_P = k_P k_{ISC} I_{EX}[MG](k_F + k_{ISC})^{-1}(k_P + k_X + k_{MT}[MG])^{-1}$ for the fluorescence and phosphorescence intensities with [MG] representing methylglyoxal pressure. If this is correct, $I_F/I_P = (k_F/k_P)(k_P + k_X + k_{MT}[MG])/k_{ISC}$. Thus a plot of I_F/I_P against [MG] should yield a straight line. Such a plot, shown in Figure 7, is indeed linear for $1.0 \leq [MG] \leq 15.0$ Torr. The ratio of slope to intercept gives $k_{MT}(k_P + k_X)^{-1} = 3.0 \pm 1.3$ Torr^{-1}. Some deviation from linearity below 1.0 Torr may be present. This would indicate lack of validity of the simple kinetic scheme in this pressure range. One possibility for such a deviation is simple molecular diffusion of triplet molecules out of the viewing range of the detection apparatus.

Assuming an initial δ function excitation pulse, the observed decay rates for fluorescence and phosphorescence are $k_{obsd,F} = k_F + k_{ISC}$ and $k_{obsd,P} = k_P + k_X + k_{MT}[MG]$. Thus, the phosphorescence decay rate should show Stern-Volmer behavior as observed (Figure 4) and the fluorescence decay rate should be pressure independent. From the data of Figures 4 and 5 we have $k_F + k_{ISC} = 4.9 \times 10^7$ sec^{-1}, $k_P + k_X = 0.52 \times 10^3$ sec^{-1}, and $k_{MT} = 1.57 \times 10^3$ sec^{-1} Torr^{-1}. Thus the time-resolved data give $k_{MT}(k_P + k_X)^{-1} = 3.02$ Torr^{-1}, in excellent agreement with the value obtained from steady state intensity measurements. Also from the values of k_{MT} and $(k_{ISC} + k_F)$ determined from time-resolved data and the slope of the I_F/I_P vs. [MG] plot we may deduce that $k_F/k_P \cong 2.3 \times 10^3$ (assuming $k_{ISC} \gg k_F$). This is very reasonable since the values of k_F and k_P are expected to be ~10^5 sec^{-1} and ~10^2 sec^{-1}, respectively.[3,23]

Several important assumptions are tacit in the kinetic scheme presented. (1) The $S_1 \rightsquigarrow T_1$ intersystem crossing rate is assumed to be irreversible. Recent results suggest that this is not the case for biacetyl at very low pressures,[7] but that it is effectively correct for pressures above 1 Torr. A similar situation exists in methylglyoxal and will be discussed elsewhere. (2) The S_1-T_1 intersystem crossing rate constant, k_{ISC}, is assumed to be constant for the limited excitation wavelength region 4400-4500 Å. The steady state excitation wavelength (4350-4450 Å) differs by ~200-400 cm^{-1} from the luminescent decay excitation wavelength (4492 Å), but in the analysis only one value of k_{ISC} is assumed. In actuality this rate constant is expected to vary only slightly in accordance with an "energy gap" law.[24] An approximately linear variation of the rate constant with increasing vibrational energy has been observed in biacetyl[6] (~7% change for 400 cm^{-1} vibrational energy). A similar dependence might be expected for methylglyoxal. (3) Vibrational excitation in T_1 formed by intersystem crossing from S_1 has been ignored. The simplified kinetic model presented here is not rigorous in that S_1 does not undergo transitions directly to those vibrational levels of T_1 associated with the observed phosphorescence but to levels containing ~3000 cm^{-1} of vibrational excitation. However, as argued by Moss and Yardley,[7] at the pressures employed vibrational relaxation should effectively couple these higher vibrational levels with the lower ones. Thus the observed phosphorescence decay processes and emission intensity may be attributed to the vibrationally equilibrated triplet manifold. (4) Vibrational equilibration in S_1 has been ignored. The slight dependence of the observed fluorescent decay times with pressure may be the result of electronic quenching (with a very small cross section) or, more likely, of vibrational equilibration. Initially a "single" vibronic level of S_1 (at 4492 Å) is excited. At low pressure only fluorescing photons from this one level are observed. At higher pressures, however, this initial excitation energy is distributed to other vibrational levels and some sort of "average" intersystem crossing rate constant, k_{ISC}, is observed. Effects of vibrational equilibration on the fluorescent lifetime have been observed in biacetyl[6] and in methyltriazolinedione.[25] The reason why the vibrational effects are observed in fluorescence but not in phosphorescence lifetime behavior is that at the pressures employed fluorescent decay paths are competitive with the collisional processes and the phosphorescent decay paths are not.

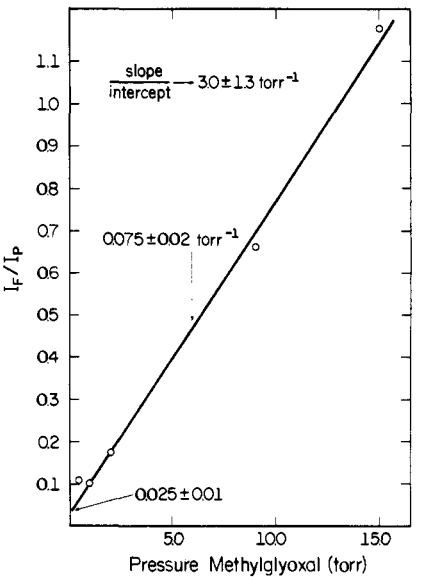

Figure 7. Ratio of the areas under the fluorescence and phosphorescence emissions (I_F/I_P) vs. methylglyoxal pressure. The ratio of the slope to intercept gives the value of $k_{MT}(k_P + k_X)^{-1}$ (see text).

Acknowledgment. We would like to thank Clif Dykstra for obtaining some low- and high-resolution spectra and Dr.

J. Lombardi for use of his high-resolution spectrometer. The continued support of the National Science Foundation is hereby gratefully acknowledged. One of us (J.T.Y.) is indebted to the Camille and Henry Dreyfus Foundation for a Teacher-Scholar Award.

Supplementary Material Available. A partial listing of absorption features in high resolution spectrum of methylglyoxal will appear following these pages in the microfilm edition of this volume of the journal. Photocopies of the supplementary material from this paper only or microfiche (105 × 148 mm, 24× reduction, negatives) containing all of the supplementary material for the papers in this issue may be obtained from the Journals Department, American Chemical Society, 1155 16th St., N.W., Washington, D.C. 20036. Remit check or money order for $3.00 for photocopy or $2.00 for microfiche, referring to code number JACS-75-1667.

References and Notes

(1) J. T. Yardley, G. W. Holleman, and J. I. Steinfeld, *Chem. Phys. Lett.*, **10**, 266 (1971).
(2) J. T. Yardley, *J. Chem. Phys.*, **56**, 6192 (1972).
(3) L. G. Anderson, C. S. Parmenter, and H. M. Poland, *Chem. Phys.*, **1**, 401 (1973).
(4) R. A. Beyer, Thesis, University of Colorado, 1973, unpublished.
(5) J. G. Calvert and J. N. Pitts, Jr., "Photochemistry", Wiley, New York, N.Y., 1966, p 323-336.
(6) G. M. McClelland and J. T. Yardley, *J. Chem. Phys.*, **58**, 4368 (1973).
(7) A. Z. Moss and J. T. Yardley, *J. Chem. Phys.*, **61**, 2883 (1973).
(8) E. Drent, R. P. Van der Werf, and J. Kommandeur, *J. Chem. Phys.*, **59**, 2061 (1973).
(9) R. P. Van der Werf, D. Zevenhuijzen, and J. Kommandeur, *Chem. Phys. Lett.*, **27**, 325 (1974).
(10) B. J. Finlayson, J. N. Pitts, Jr., and R. Atkinson, *J. Am. Chem. Soc.*, **96**, 5356 (1974).
(11) J. Lombardi, *J. Chem. Phys.*, **50**, 3780 (1969).
(12) C. A. Thayer and J. T. Yardley, *J. Chem. Phys.*, **57**, 3992 (1972).
(13) J. T. Yardley, "Dynamic Properties of Electronically-Excited Molecules", in "Chemical and Biological Applications of Lasers", C. B. Moore, Ed., Academic Press, New York, N.Y., 1974.
(14) E. Drent and J. Kommandeur, *Chem. Phys. Lett.*, **14**, 321 (1972).
(15) S. P. McGlynn, T. Azumi, and M. Kinoshita, "Molecular Spectroscopy of the Triplet State", Prentice-Hall, Englewood Cliffs, N.J., 1969, p 84.
(16) (a) R. Hoffmann, *Acc. Chem. Res.*, **4**, 1 (1971); (b) J. R. Swenson and R. Hoffmann, *Helv. Chim. Acta*, **53**, 2331 (1970).
(17) J. W. Sidman and D. S. McClure, *J. Am. Chem. Soc.*, **77**, 6461 (1955).
(18) J. F. Arnett, G. Newkome, W. L. Mattice, and S. P. McGlynn, *J. Am. Chem. Soc.*, **96**, 4385 (1974).
(19) J. Kelder, H. Cerfontain, J. K. Eweg, and R. P. H. Rettschnick, *Chem. Phys. Lett.*, **26**, 491 (1974).
(20) K. Kaya, W. R. Harshbarger, and M. D. Robin, *J. Chem. Phys.*, **60**, 423 (1974).
(21) J. Paldus and D. A. Ramsay, *Can. J. Phys.*, **45**, 1389 (1967).
(22) J. P. Byrne and J. G. Ross, *Aust. J. Chem.*, **24**, 1107 (1971).
(23) H. W. Sidebottom et al., *J. Am. Chem. Soc.*, **94**, 13 (1972).
(24) S. F. Fischer and E. C. Lim, *Chem. Phys. Lett.*, **26**, 312 (1974).
(25) A. V. Pocius and J. T. Yardley, *J. Chem. Phys.*, **61**, 3587 (1974).

Cadmium-113 Fourier Transform Nuclear Magnetic Resonance Spectroscopy

Alan D. Cardin,[1] Paul D. Ellis,* Jerome D. Odom,* and James W. Howard, Jr.

Contribution from the Department of Chemistry, University of South Carolina, Columbia, South Carolina 29208. *Received August 22, 1974*

Abstract: Cadmium-113 pulsed Fourier Transform nmr studies have been carried out on a variety of ^{113}Cd-metal-containing systems. It has been shown that millimolar concentrations of ^{113}Cd are readily adaptable for chemical shift and T_1 studies. Furthermore, the chemical shift range for ^{113}Cd exceeds 640 ppm which is consistent with large paramagnetic contributions to the shielding constant. As much as 300 ppm of this chemical shift range can be attributed to substituent effects, which occur in ^{113}Cd organometallic compounds. In addition to these findings, certain dialkylcadmium compounds have been shown unequivocally to undergo homoexchange with an upper limit to the rate constant of 4.5×10^2 sec^{-1} for the self-exchange process. Organic solvent interactions also play a major role in affecting the chemical shift range and the rates of exchange processes in dialkylcadmium compounds. A discussion of data concerning ^{113}Cd spin-lattice relaxation times is presented. It has been determined that spin-relaxation times in inorganic and organocadmium compounds arise from a variety of competing mechanisms.

Nuclear magnetic resonance studies of metals by methods of direct observation have not received the same level of scrutiny that nuclei such as ^{1}H, ^{19}F, and ^{13}C have received. There are a number of factors attributable, a few being (a) the inherent sensitivity associated with a particular metal isotope as compared to an equal number of protons, (b) the percentage of a naturally occurring metal isotope, (c) the associated quadrupolar moments of metal nuclides for which $I > \frac{1}{2}$ and, (d) commercial spectrometers which are unable to meet the stringent requirements necessary for metal observation.

In view of these problems, however, the literature contains a considerable amount of work involving metal systems. A significant fraction of early studies employed wide-line spectrometers and rapid passage techniques. The reader is referred to several reviews which deal, in brevity, with some of these earlier studies.[2-4] INDOR has proven to be a superior technique to CW methods previously employed and more recent studies[5-19] involving double resonance techniques are being utilized in order to gain more insight into metal-containing systems. INDOR, however, is limited at best in that its applicability requires indirect spin coupling to a nucleus having a large magnetic moment. Therefore, systems of solvated metal ions do not fall within the realm of investigation by this technique. Nor is it applicable when ^{1}H decoupling or studies involving time-dependent phenomena, such as dynamic nuclear polarization, reaction kinetics, and nuclear relaxation measurements, are to be employed.

Those metals, such as ^{113}Cd, ^{119}Sn, ^{199}Hg, ^{205}Tl, and ^{207}Pb, whose inherent nuclear properties are comparable to ^{13}C (i.e., $I = \frac{1}{2}$, sensitivity and natural abundance) could be investigated with the same experimental techniques presently employed for ^{13}C, i.e., pulsed Fourier Transform (FT) nmr. A number of researchers[20-29] have addressed themselves to just such an approach from both a variable field and a variable frequency standpoint. Variable frequency has the advantage of the employment of heteronuclear decoupling. A summary of some of these techniques can be found in recent reviews.[30,31]